Measuring Intraocular Pressure Using Soundwaves from a Smartphone

Matthew Soanes [a], Khamis Essa [a], Dr. Haider Butt [a,b]

[a]*School of Engineering, University of Birmingham, Edgbaston, Birmingham B15 2TT, UK.*

[b]*Department of Mechanical Engineering, Khalifa University, Abu Dhabi 127788, UAE*

Keywords: intraocular pressure, glaucoma, ocular hypertension, acoustic reflection coefficient

1. Abstract

Early detection of increasing values of intraocular pressure (IOP) due to glaucoma can prevent sever ocular diseases and ultimately, prevent loss of vision. Currently, the need for an accurate, mobile measurement of intraocular pressure is unmet within the modern healthcare practices. There is a potential to utilize soundwaves as a mobile measurement method and therefore, the relationship between IOP and the reflection coefficient of sound waves is investigated. Simulations are conducted using COMSOL Multiphysics to provide theoretical confirmation of the worthiness of the experiment. An experimental demonstrated is presented to further investigate the relationship between the internal pressure of an object and its acoustic reflection coefficient. The experiment exploits the use of hydrostatic pressure to determine internal pressure, and the reflection coefficient is measured and analyzed. An initial experiment is conducted to identify the resonant frequency of the object and the optimal frequency for maximizing reflection. The experiment shows comprehensively that there is a relationship between the internal pressure of an object and its acoustic reflection coefficient, providing a confirmation of the theory that would allow mobile measurements of IOP to be conducted with the use of a smart phone.

2. Introduction

The human eye is a very sensitive and cherished organ for its unparalleled use for humans on a daily basis. Thus, its continued state of health is of upmost importance to individuals worldwide. Some of the most common eye related diseases are often avoidable and display strong risk factors some time before their onset. For example, in the case of diabetic retinopathy, individuals with diabetes are specifically at risk and so are constantly monitored for background retinopathy, tiny bulges that develop in the blood vessels of the eye.[1] However, in the case of glaucoma, an ocular disease with age and elevated levels of IOP as significant risk factors, it is harder to specify such a specific group of individuals at risk of development. For this reason, an accurate, non-invasive, mobile measurement of IOP would provide a means to continuously monitor an individual's IOP over long dura. This would lead to earlier diagnosis and treatment of the condition, drastically increasing the chances of maintaining the individual's vision.

IOP is a vital measurement in the continued healthy state of the human eye. It is defined as "the pressure created by the continued renewal of fluids within the eye",[2] where a healthy value between $10 - 20\ mmHg$ is essential to maintain the conditions for optimal refraction.[3] An inflated IOP is referred to as ocular hypertension and is caused by an imbalance in the production and drainage of aqueous fluid in the eye. This imbalance is most common in older adults, with the risk increasing as you get older and in turn, increasing the risk of the patient developing Glaucoma. Glaucoma is a disease of the optic nerve which affects 64.3 million people worldwide as of 2013,[4] if left untreated it causes irreversible damage to the nerve and loss of sight. The difference between a healthy eye and a glaucoma inflected eye is shown in **Figure 1e**.

The current, 'gold standard' method of measurement of IOP is applanation tonometry,[5] namely Goldmann (slit lamp) or Perkins (handheld), as illustrated in **Figure S1a and S1b**. This works on the Imbert-Fick law, which states that "the force required to flatten or applanate a sphere (W) is equal to the product of the pressure inside the sphere (P) and the area applanated (A): W=P×A".[6] In practice, numbing drops followed by non-toxic dye are applied to the patient's eyes. This

provides the base for the measurement which is gathered by a small tip indenting a small area of the cornea,[7] and the required force for this measured. Although this is considered 'gold standard', it does arise with problems and in turn, errors in measurement.

An independent risk factor of glaucoma is having a thin central corneal thickness (CCT),[7] which is a transparent layer forming the front of the eye. This can be caused by natural occurrence, or a common procedure like laser eye surgery. However, a thin CCT also causes artificially low readings of IOP when using applanation tonometry,[5] which has been recorded as a difference of as much as $0.32\ mmHg$ per $10\ \mu m$ change in CCT.[6] The only way to decipher whether the reading is artificial, or healthy and correct is by a full eye examination including a measurement of CCT, rendering an isolated, mobile applanation measurement of IOP (Perkins) useless. Furthermore, a Perkins tonometer is too expensive to be accessible for purchase by the majority of the population for home usage for prolonged IOP monitoring.

Even a Goldmann-type tonometer reading of IOP can cause large errors, found experimentally to be as much as $5\ mmHg$.[8] Considering the cut-off level of IOP that differentiates normal and abnormal is widely considered $21\ mmHg$,[8] this equates to a 23.8% error, which is unacceptable.

Pneumotonometry is another applanation method of measuring IOP which is less influenced by CCT [5] and is non-contact. An experiment shows there was no 'statistically significant differences in IOP as a function of change in corneal thickness or change in corneal curvature'.[9] It utilizes a floating pneumatic sensor that touches the cornea and records a measurement of IOP.[10] Usually slightly lower than Goldmann, provided the Goldmann measurement is not artificially low. In a professional setting, these values should still be treated cautiously.

A pneumotonometry form of IOP measurement is air-puff tonometry, **Figure S1c**, which utilizes a rapid air pulse to applanate the cornea. When this is done, an infrared light beam is reflected off the flattened surface of the cornea.[10] In essence this is a similar method as applanation, however, it achieves a measurement without the need for contact with the eye and, therefore, the numbing drops or dye. Air-puff tonometry is considered less accurate as it gives a higher reading of IOP in 74% of

patients,[10] as shown by experimental evidence. It is also considered 'uncomfortable' and 'unpleasant' by some patients.[11]

As well as problems of discomfort and invasion, the diurnal fluctuation is the varying of IOP throughout the course of a single day [12] and is caused by hormonal effects on the eyes. This, in turn, causes problems in ensuring accurate measurement. Generally, IOP is higher in the morning for any one individual however the level of increase cannot be calculated. Therefore, for an accurate measurement to be taken, hourly measurements must be taken to monitor the range of the diurnal fluctuation throughout the day. This is very impractical for the discussed methods, as they must all be completed externally at an optician's and completed by a professional. For an accurate daily measurement to be taken practically, a simple, mobile measurement must be available of which there is only one method in use, rebound tonometry.

Rebound tonometry, **Figure S1d**, is employed as a method that is 'well tolerated and safe',[13] so is suitable for children and pets. It is undertaken by a handheld device so it can be used in homes and does not require anaesthetic or staining dye. It works via a tiny plastic ball being fired rapidly at the cornea, and its deceleration when they come in to contact correlating to a recorded IOP. The larger the deceleration, the higher the IOP. The plastic ball is attached to the end of a stainless-steel wire and held in place by an electromagnetic field until released.[14] However, initial experiments show that although it is a weak correlation, it shares a similar relationship with the central corneal thickness (CCT) with that of Goldmann applanation tonometry, which can result in artificially low values as previously discussed. It also requires the instrument to be kept upright and kept at the correct distance from the cornea, therefore mobile measurements can prove problematic.[15] Similarly to the Perkins tonometer, a rebound tonometer is very expensive with prices starting at £1,595.[16]

The improved, mobile method being proposed will involve a simple procedure of firing sound waves at the eye from a predefined incident angle and measuring the coefficient of reflection. It will be conducted using a smartphone, which is widely accessible with over half of 65+ adults in

America already owning one, a figure which will only increase in the future as the current population grows older (50-64, 79% ownership, 65+, 53% ownership).[17] In contrast to the previously discussed methods, it would be accessible, comfortable and simple to perform mobile readings. Furthermore, as this method does not applanate the surface of the eye CCT should not have any effect on the reflection coefficient. With all these factors taken into consideration, if the method is implemented, it will be far superior to any of the current methods of IOP measurement.

2. Modeling

The experiment proposed will investigate if the internal pressure of an eye-replicating object affects the reflection coefficient of acoustic waves. To validate the worthiness of experimentation, modeling software Comsol Multiphysics was utilized to prove a basic relationship between the reflection coefficient and IOP of the eye. Comsol is used as it is a validated and trusted simulation software for reflection coefficient simulations.[18]

2.1 Model Construction

The model was constructed using a computational geometry to simulate an average human eye. Table 1 shows the geometry used for the simulation model and is based on an average between male and female values from literature. The 2D model is illustrated in **Figure 2a**. A 210° revolution image of the model is shown in **Figure 2b.** The model was constructed as a half-body model to exploit the 2D axisymmetric nature of the human eye and reduce computational time.

Knowledge of accurate precorneal tear film thickness is limited, with no consensus on the true value. Invasive methods have produced estimates in the range $4 - 10\ \mu m$, this range is further supported by reflection spectra showing a peak at similar values.[19] Thus, the value of $5\ \mu m$ was estimated. Precorneal tear film structure consists of an inner mucus layer and an outer oily layer; however, the structure is dominated by the middle aqueous layer which is mostly water and dissolved nutrients.[20] Therefore, for the simulation, the precorneal tear film layer was modeled as a water layer using the embedded software properties for water at room temperature.

As the geometry is curved, a perfectly matched layer could not be utilized to represent the open space. Thus, the boundaries were modeled as artificial boundary layers to simulate an open cavity as they do not represent physical walls.

The sound waves can be assumed as high frequency ($\geq 2000\ Hz$) and highly localized due to the production of the sound wave from a local source. With these conditions, the sound source can be modeled as a Gaussian pulse (a pulse with the temporal shape of a Gaussian distribution) of $1\ mm$ radius.[21, 22] The use of a high frequency sound nullifies the material thickness effect on absorption that affects low frequency incident sound waves.[22] The incident pressure field was defined as cylindrical wave radiation as this allows the pressure wave to leave the domain without spurious reflections based on the conditions of the simulation.[23] During the simulation, the sound waves will be reflected off the center of the cornea, thus a constant corneal thickness is assumed, although in reality, the thickness increases towards the periphery.[24] In addition, it also assumed that there will be no reflection from the retina, isolating the reflections from the cornea.

Using the acoustics module within Comsol Multiphysics, IOP could not be explicitly input as a parameter, thus, the relationship between IOP and a physical parameter that exploits the governing equations of the Pressure Acoustics, Frequency Domain was established.[25]

Previous experiments for a wide range of applications have estimated the porosity of a material using its pressure, as in a lot of cases it is easier to measure pressure variations in changing conditions. As a result of this, many have formulated relationships estimating the porosity of a material using pressure, showing there is a relationship between the two parameters.[26-29] Porosity is a parameter that can be explicitly used as a dependent variable in Comsol Multiphysics, thus it can be used to prove an implicit relationship between pressure and reflection coefficient.

Porosity is a value between 0-1 that represents a fraction of the volume of pores in a material compared to total mass volume, usually ranging up to a maximum value of over 0.5 for peat or clay.[30] For this reasoning, the porosity values were ranged from 0.1 to 0.6 to verify the relationship

between porosity and reflection coefficient. Parameters input into Comsol Multiphysics are outlined in Table 2.

2.2 Results

The geometry and parameter set up allowed an accurate model to be created and allowed a sweep of frequency and porosity. This was used to obtain results confirming the relationship between pressure and reflection coefficient. The results are shown in **Figure 2c**. Figure 2c shows that at lower frequencies ($< 6000\ Hz$) the reflection coefficient shows a positive correlation with the material's porosity, and thus the pressure. A porosity value of 0.2 showed an anomaly at a frequency of $2000\ Hz$ with a largely inflated value, likely due to inaccuracies of the modeling software at lower frequencies. As the frequency was increased in the range $6000 - 20000\ Hz$, the reflection coefficient converged to a reflection coefficient of 0, rendering these frequencies useless for experimentation. Due to the convergence to 0, Figure 2c only shows the results up to $16000\ Hz$. Figure 2c shows that the most variation in reflection coefficients between porosity values is evident at a driving frequency of $4000\ Hz$, and thus, this will be investigated further. **Figure 2d** shows the relationship between porosity and reflection coefficient at a driving frequency of $4000\ Hz$, showing a significant positive correlation. This confirms the relationship between IOP and reflection coefficient, validating the worthiness of conducting the experiment. It can be conceded that the quality of the results shown in Figure 2c are not excellent, due to the convergence of the results and the variation in relationships shown at different porosities. However, due to Figure 2d showing a very clear relationship, this was considered as justification to conduct the physical experimentation.

3. Experimental

3.1 Theory

To investigate the relationship between IOP and the reflection coefficient, an experiment was conducted. The experiment involved the application of the hydrostatic pressure theory to determine the pressure inside an object replicating the human eye. Hydrostatic pressure is defined as "The pressure exerted by a fluid at equilibrium at a given point within the fluid, due to the force of gravity. Hydrostatic pressure increases in proportion to depth measured from the surface because of the increasing weight of fluid exerting downward force from above." [31] It follows the relationship shown by Equation 1.

$P = \rho g h$ [31] (1)

Where:

P = Pressure in liquid at depth h $[Pa]$

ρ = Density of fluid (water) = $1000\ kg.m^{-3}$

g = Gravitational constant = $9.81\ m.s^{-2}$

h = Depth in fluid $[m]$

97.5% range of human eye pressure varies between $7.3 - 22.1\ mmHg$,[32] equating to approximately $950 - 2950\ Pa$. Solving for h (Equation 1), this is a variation in depth of approximately $0.10 - 0.30\ m$. The measurement at a water depth of $0.30\ m$ represents the reading of an eye with ocular hypertension.

Sound waves fired at the eye will experience a portion of the wave that will aim to pass through the medium, whereas the remaining wave energy will reflect off the medium at an angle equal to the angle of the incident wave, as illustrated by **Figure 3a**.[33] The reflection coefficient of the medium is defined as the ratio of the reflected wave to incident wave amplitudes and is a relationship commonly exploited in ultrasound applications.[34]

The material properties for the eye replicating object in the experimental method will dictate the resonant frequency of the object. At resonance, the absorption of the material is maximum and the reflection coefficient will become problematic to analyze.[35] For these reasons, an initial frequency sweep was performed at a constant pressure to identify the resonant frequency of the object and ensure it is avoided in further experimentation.

The geometry of incident surfaces is exploited in acoustics in conjunction with material properties to significantly alter the reflection of sound waves in applications such as soundproofing rooms and optimising sound quality in recording studios. Therefore, it is essential that the geometry of the replica eye remains constant throughout the experimentation to nullify the effect.

3.2 Results & Discussion

Figure 4a shows the frequency spectrum produced on Audacity for a driving frequency of $2000\ Hz$. The subsequent peaks after the largest at $2000\ Hz$ are all at intervals of 2000 due to the waves being harmonics of each other, shown by **Figure 4b**. This shows the first seven harmonics, which for the $2000\ Hz$ incident wave frequency represents the peaks up to and including $14000\ Hz$.

This confirms that Figure 4a matches the theoretical frequency spectrum for an incident wave frequency of $2000\ Hz$, and this trend continues for all frequency analysis conducted on Audacity. It is confirmed from this that there was negligible background noise interference in any of the sound recordings during the experiments. Figure 4a also confirms the accuracy of the application used to generate the sound waves, 'Tone generator'.

Table 3 shows the results for the frequency sweep and is illustrated by **Figure 5a**. From these results it can be concluded that the resonant frequency for the replica eye is at $11000\ Hz$ and the optimal frequency for maximizing reflection is $8000\ Hz$. The results confirm the theoretical pattern, where there is a frequency ($11000\ Hz$) which represents the resonant frequency of the material and absorption increases to a much higher value than at surrounding frequencies. There is

also a frequency ($8000\ Hz$) where reflection is maximum, matching theoretical expectations. For these reasons, the results from the initial frequency sweep can be assumed as accurate.

With the optimal driving frequency determined, the incident wave amplitude was determined by firing an $8000\ Hz$ sound wave directly at the microphone at the same distance as the reflected waves, resulting in a sound level of $-16.6\ dB$. Supplementary results used to calculate an average for calculations to populate Table 5 are shown in **Table 4**. The standard deviation values provide an indication to the spread of the data, relatively low in this experiment. The standard deviations are increased by relatively higher values for all readings in the first completion of the experiment, shown in Table 4. However, all of the completions of the experiment showed the same relationship, so the elevation of the first set was considered as unimportant in the context of the experiment.

The reflection coefficients in Table 4 were calculated using Equation 2.

$$R_C = \left(\frac{A_R}{A_I}\right)^{-1} = \frac{A_I}{A_R} \qquad (2)$$

Where:

R_C= Reflection coefficient

A_R= Average sound level of reflected wave (Table 4)

A_I= Sound level of incident wave= $-16.6\ dB$

Note the sound level values in Audacity are negative as the reference is a zero value, representing the maximum sound level possible for analysis on Audacity before distortion. This is the reason for Equation 2 being inverted, with its more common form being applicable to positive values of sound level.

The data in Table 5 is illustrated in **Figure 5b**. The results show that as the internal pressure of an object increases, the reflection coefficient increases. Initially the increase shows a linear fashion, at a rate of approximately $1.80\ R_C.mmHg^{-1}$ through the range $0.100 - 0.200\ m$, however this rate decreases and begins to plateau as the pressure increases above a depth of $0.250\ m$. It can be comprehensively concluded from this that there is a relationship between internal pressure of an

object and its acoustic reflection coefficient, when other parameters are kept constant. Although this confirms there is a relationship, being able to accurately measure IOP using sound waves from a mobile device may prove difficult due to the relatively small increase in R_C for the increase in IOP. It could however be very useful in the monitoring of an individual's IOP, and flag up when the individual experiences an increase in IOP if it were to be monitored consistently over a period of time.

The reflection coefficients shown in Table 5 may be inflated as there was nothing preventing some soundwaves traveling directly from the source, to the microphone without reflecting off the object. As the sound level of the source and the positioning of the source and microphone were invariable, it was assumed that the inflation as a result of this would be the same for all readings of wave amplitude. Thus, it would not cause a misinterpretation of the relationship.

Following on from the results of this experiment, it is evident that the plateauing of results occurs towards the pressure range indicating hypertension in a patient's eyes. As this could be due to the relatively larger values of reflection coefficient at a driving frequency of $8000\ Hz$, shown in Figure 5a, a further experiment was conducted at a driving frequency of $6000\ Hz$ to investigate if this would avoid, or delay, the plateauing effect. The experiment was conducted in an identical manor to the experiment previous, apart from the change to the driving frequency and the depth of water range was increased to $0.10 - 0.40\ m$ to investigate the pressures beyond ocular hypertension. The baseline sound level recorded was $-16.0\ dB$. The associated results are given in **Table 6** and **7**, and the reflection coefficient vs depth of water graph is shown in **Figure 5c**.

As can be seen from these results, the same relationship is shown, with an increase in internal pressure causing an increase in reflection coefficient. The plateauing effect is delayed to values beyond those indicative of ocular hypertension, however the gradient of the relationship is smaller than previous. As the measurement of discrete differences in IOP was already a concern, this further reduction may render accurate measurements unattainable by individuals. **Figure 5d** shows a graph comparing the reflection coefficient of the sound waves for both incident wave frequencies of

6000 & 8000 Hz. The red line represents the depth of water indicating ocular hypertension, 0.285 m. This value was calculated using Equation 1 and a pressure value of 22.1 $mmHg$ (2800 Pa).[8] Figure 5d clearly shows the delay in the plateauing of results past the hypertension indicative red line for a 6000 Hz driving frequency. However, as previously discussed, despite delaying a complete plateauing, the increase in reflection coefficient may not be sufficient to be accurately measurable.

3.3 Method

The depth of water was varied using a graduated water tower with a nozzle at the lower end for attachment of the replica eye shown in **Figure 3b**. The replica eye used was a latex balloon housed in plastic tubing, due to its benefit of retaining its geometry with varying levels of pressure. Sound waves were generated using a smartphone (iPhone 8) application 'Tone generator', with the lower right speaker being isolated for the experiment.[36] A Zoom U-44 Handy Audio Interface and an sE SE1A microphone were used in conjunction with computer software Audacity as an oscilloscope to analyze the sound waves. Images of the equipment used are shown in **Figure S2**. The equipment was set up as shown in Figure 3a, ensuring the reflected wave is directed towards the center of the microphone. **Figure 3c** and **3d** show further views of the apparatus setup. The sound wave source and microphone were both placed a distance of at least one wavelength away from the reflection boundary, which is a distance of 0.172 m for the minimum frequency of 2000 Hz, using Equation 3.

$$\lambda = \frac{c}{f} \quad (3)$$

Where:

$\lambda =$ Wavelength $[m]$

$c =$ Speed of sound at sea level $= 344\ m.s^{-1}$

$f =$ Frequency $[Hz]$

To conduct the experiment, the sound wave was exposed to the material for approximately two seconds. This allowed ample time for Audacity to provide a stabilized sound pattern for analysis. The frequency sweep was conducted by increasing the frequency from $2000 - 16000\ Hz$ in $1000\ Hz$ increments. The results of the peak amplitude at the driving frequencies are shown in **Table 3**. The sweep was conducted using an incident wave angle (θ) of 30° and a water depth (h) of $0.175\ m$.

The internal pressure of the replica-eye was increased by increasing the water depth from $0.10 - 0.30\ m$ in $0.025\ m$ increments. The incident wave angle was again set at 30°. The results are shown in **Table 5**.

4. Conclusion

In conclusion, a relationship was confirmed between internal pressure and acoustic reflection coefficient. The aim was met comprehensively through physical experimentation, which showed a clear increase in the reflection coefficient as the internal pressure of an object increased at a rate that is measurable for mobile equipment. Critical frequencies were also discovered for effective measurement of reflection coefficient at pressure values that surpass those of ocular hypertension. In practise, the critical frequency value for human eyes must be determined through experimentation using a method similar to that completed in this report and analyzed for suitability. Although the relationship confirmed achieved the aim of the project, the investigation was performed whilst keeping other material properties consistent, most notably the geometry of the object. Geometry is a property that is different for all individuals and is also a property that has a significant effect on sound wave reflections. Thus, it is probable that sound waves could accurately be used to measure IOP if the geometry of the eye is known. Further investigation should be conducted into the accurate, mobile measurement of eye geometry, rendering a complete eye pressure measurement achievable. For this to be an accurate measurement, an investigation should be conducted to quantify the changes in eye geometry and how this impacts the value of the

reflection coefficient. If this is achieved, it is fully viable for an accurate, mobile measurement of IOP to be conducted using a smartphone, from the comfort of the user's home.

References

[1] Semeraro F, Cancarini A, dell'Omo R, Rezzola S, Romano M, Costagliola C. *Diabetic Retinopathy: Vascular and Inflammatory Disease. Journal of Diabetes Research.* **2015***, Vol: 2015, Page:1-16.*

[2] MedicineNet, Medical Definition of Intraocular pressure. https://www.medicinenet.com/script/main/art.asp?articlekey=4014, accessed September, 2019.

[3] Wang YX, Xu L, Wei WB, Jonas JB. *Intraocular pressure and its normal range adjusted for ocular and systemic parameters. The Beijing Eye Study 2011.* **2018,** *Vol: 13, Issue: 5*

[4] Yih-Chung Tham, Xiang Li, Tien Y. Wong, Harry A. Quigley, Tin Aung, Ching-Yu Cheng. *Global Prevalence of Glaucoma and Projections of Glaucoma Burden through 2040. Ophthalmology, ISSN: 1549-4713*, **2014,** *Vol: 121, Issue: 11, Page: 2081-90*

[5] BrightFocus Foundation. How is Eye Pressure Measured? BrightFocus Foundation. https://www.brightfocus.org/glaucoma/article/how-eye-pressure-measured#:~:text=Your%20ophthalmologist%20will%20instruct%20you,fixed%20area%20of%20the%20cornea, accessed September, 2019.

[6] Sunil Shah. *Accurate intraocular pressure measurement-the myth of modern ophthalmology? Ophthalmology, ISSN: 0161-6420,* **2000,** *Vol: 107, Issue: 10, Page: 1805-7*

[7] *Charles W. McMonnies. Glaucoma history and risk factors J Optom* **2017,** *2016 71-78*

[8] Sean McCafferty, Jason Levine, Jim Schwiegerling, Eniko T. Enikov. *Goldmann applanation tonometry error relative to true intracameral intraocular pressure in vitro and in vivo. BMC Opthalmology.* **2017,** *Vol: 17, Issue: 1, Page: 215*

[9] David Zadok, Dan B Tran, Michael Twa, Miriam Carpenter, David J Schanzlin. *Pneumotonometry versus Goldmann tonometry after laser in situ keratomileusis for myopia. Journal of cataract and refractive surgery*, ISSN: 0886-3350, **1999**, *Vol: 25, Issue: 10, Page: 1344-8.*

[10] Carlos Gustavo V. De Moraes, Tiago S. Prata, Jeffrey Liebmann, Robert Ritch. *Modalities of Tonometry and their Accuracy with Respect to Corneal Thickness and Irregularities. J Optom.* **2008**, *Vol: 1, Issue: 2, Page: 43-49*

[11] Qasim K Farhood, *Comparative evaluation of intraocular pressure with an air-puff tonometer versus a Goldmann applanation tonometer. Clin Ophthalmol.* **2013**, *Vol: 7, Page: 23-27*

[12] ESSILOR NEWS. THE EYE AIR PUFF TEST - WHY YOU CAN'T HIDE FROM IT. https://www.essilorusa.com/newsroom/the-eye-air-puff-test-why-you-cant-hide-from-it (accessed October 2019)

[13] Glaucoma NZ. *Your Glaucoma Eye Examination: Part 1.* **2008** *Vol: 5, Issue: 1.*

[14] Iliev ME, Goldblum D, Katsoulis K, Amstutz C, Frueh B. *Comparison of rebound tonometry with Goldmann applanation tonometry and correlation with central corneal thickness. Br J Ophthalmol*, **2006**. *Vol: 90, Issue: 7, Page: 833-835*

[15] S Nakakura. *Icare rebound tonometers: review of their characteristics and ease of use. Clinical Ophthalmology*, **2018**, *Vol: 12, Page: 1245-1253*

[16] NICE Pathways, Icare rebound tonometer to measure intraocular pressure, https://www.nice.org.uk/advice/mib57, accessed October, 2019.

[17] Pew Research Centre. Mobile Fact Sheet. https://www.pewinternet.org/fact-sheet/mobile/, accessed October, 2019.

[18] Comsol Application Gallery. Acoustic Reflection Analyser for a Water-Sediment Interface. https://uk.comsol.com/model/acoustic-reflection-analyzer-for-a-water-sediment-interface-30881, accessed September, 2019.

[19] Ewen King-Smith P, Fink B, Fogt N, Nichols K, Hill R, Wilson G. *The Thickness of the Human Precorneal Tear Film: Evidence from Reflection Spectra. Investigative Ophthalmology & Visual Science*, **2000**, *Vol: 41, Page: 3348-3359*

[20] Vismed.trbchemedica.co.uk. The precorneal tear film. https://vismed.trbchemedica.co.uk/business-professionals/understanding-the-tear-film/the-precorneal-tear-film, accessed January, 2020.

[21] Weik M.H. *Gaussian-shaped pulse. Computer Science and Communications Dictionary. Springer, Boston, MA.* **2017** *Vol: 2017, Issue: 1, Page: 676*

[22] S. Seddeq, H. *Factors Influencing Acoustic Performance of Sound Absorptive Materials. Australian Journal of Basic and Applied Sciences*, **2009**, *Vol: 3, Issue: 4, Page: 4610-4617*

[23] COMSOL, Theory for the Plane, Spherical, and Cylindrical Radiation Boundary Conditions https://doc.comsol.com/5.5/docserver/#!/com.comsol.help.aco/aco_ug_pressure.05.130.html, accessed January, 2020.

[24] Martola E. *Central and Peripheral Corneal Thickness. Archives of Ophthalmology.* **1968,** *Vol: 79, Issue: 1, Page: 28*

[25] COMSOL, Acoustic Module User's Guide. 2018. https://doc.comsol.com/5.4/doc/com.comsol.help.aco/AcousticsModuleUsersGuide.pdf, accessed October, 2019.

[26] M.F. de Siqueira, F. Silva, M.D. Marsili, P.S. Rocha, A. Kronbauer, C. Sisk, A. Grader, J. Toelke, and A. Jordan. *Estimation of Permeability, Porosity and Rock Compressibility Properties using Digital Rock Analysis Technique for a Heavy Oil Unconsolidated Sandstone Offshore Brazil. Search and Discovery*, **2018**, *Article #30587.*

[27] Ghabezloo S, Sulem J, Saint-Marc J. *Evaluation of a permeability porosity relationship in a low permeability creeping material using a single transient test, International Journal of Rock Mechanics and Mining Sciences*, **2009**, *Vol: 46, Issue: 4, Page: 761-768.*

[28] Kitamura K, Takahashi M, Mizoguchi K, Masuda K, Ito H, Song S. *Effects of pressure on pore characteristics and permeability of porous rocks as estimated from seismic wave velocities in cores from TCDP Hole-A. Geophysical Journal International.* **2010,** *Vol: 182, Issue: 3, Page:1148-1160*

[29] Glover P. Formation Evaluation MSc Course Notes, http://homepages.see.leeds.ac.uk/~earpwjg/PG_EN/CD%20Contents/Formation%20Evaluation%20English/Chapter%205.PDF, accessed December, 2019.

[30] Martin F, Colpitts R. *Reservoir Engineering. Standard Handbook of Petroleum and Natural Gas Engineering.* **1996**, *Vol: 2, Page: 1-362*

[31] Dictionary.com, Definition of hydrostatic pressure, https://www.dictionary.com/browse/hydrostatic-pressure, accessed January, 2020.

[32] Wang Y, Xu L, Wei W, Jonas J. *Intraocular pressure and its normal range adjusted for ocular and systemic parameters. The Beijing Eye Study 2011. PLOS ONE.* **2018**, *Vol: 13, Issue: 5*

[33] Bouzidi Y, Schmitt D. *Incidence-angle-dependent acoustic reflections from liquid-saturated porous solids. Geophysical Journal International.* **2012**, *Vol: 191, Issue: 3, Page: 1427-1440*

[34] Dukhin A, Goetz P. *Fundamentals of Acoustics in Homogeneous Liquids. Characterization of Liquids, Nano- and Microparticulates, and Porous Bodies Using Ultrasound.* **2010**, *Vol: 24, Page: 91-125.*

[35] Schwan L, Umnova O, Boutin C. *Sound absorption and reflection from a resonant metasurface: Homogenisation model with experimental validation. Wave Motion.* **2017**, *Vol: 72, Page:154-172*

[36] App Store, Tone generator 2011 https://apps.apple.com/gb/app/tone-generator/id457003837 accessed February, 2020.

[37] Rufer F, Schroder A, Erb C. *White-to-White Corneal Diameter. Cornea.* **2005**, *Vol: 24, Issue: 3, Page: 259-261*

[38] Mashige K. *A review of corneal diameter, curvature and thickness values and influencing factors. African Vision and Eye Health.* **2013**, *Vol: 72, Issue: 4*

[39] Shao, P., Seiler, T., Eltony, A., Ramier, A., Kwok, S., Scarcelli, G., II, R. and Yun, S. *Effects of Corneal Hydration on Brillouin Microscopy In Vivo. Investigative Opthalmology & Visual Science*, **2018**, *Vol: 59, Issue: 7, Page: 3020*

[40] Leonard, D. and Meek, K. *Refractive indices of the collagen fibrils and extrafibrillar material of the corneal stroma. Biophysical Journal,* **1997**, *Vol: 72, Issue: 3, Page: 1382-1387*

[41] Prausnitz, M. and Noonan, J. *Permeability of cornea, sclera, and conjunctiva: A literature analysis for drug delivery to the eye. Journal of Pharmaceutical Sciences,* **1998,** *Vol: 87, Issue: 12, Page: 1479-1488*

[42] Lee, V. *Mechanisms and facilitation of corneal drug penetration. Journal of Controlled Release,* **1990**, *Vol: 11, Issue: 1-3, Page: 79-90*

[43] Shih, P., Huang, C., Huang, T., Lin, H., Yen, J., Wang, I., Cao, H., Shih, W. and Dai, C. *Estimation of the Corneal Young's Modulus In Vivo Based on a Fluid-Filled Spherical-Shell Model with Scheimpflug Imaging. Journal of Ophthalmology,* **2017**, *Vol: 2017, Page: 1-11*

[44] Aloy, M., Adsuara, J., Cerdá-Durán, P., Obergaulinger, M., Esteve-Taboada, J., Ferrer-Blasco, T. and Montés-Micó, R. *Estimation of the mechanical properties of the eye through the study of its vibrational modes.* **2017**, *PLOS ONE, Vol: 12, Issue: 9, Page: e0183892*

[45] Bower, A. *Constitutive Models- Relations between Stress and Strain. Applied Mechanics of Solids.* **2008**. *Chapter: 3*

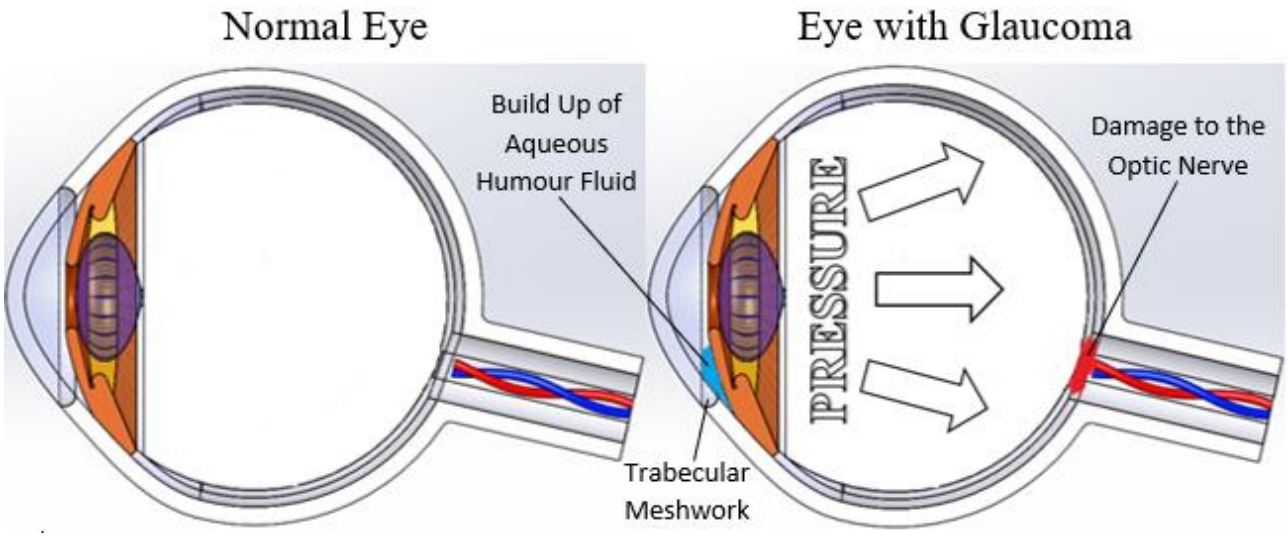

Figure 1. Comparison between a healthy eye and an eye infected with glaucoma

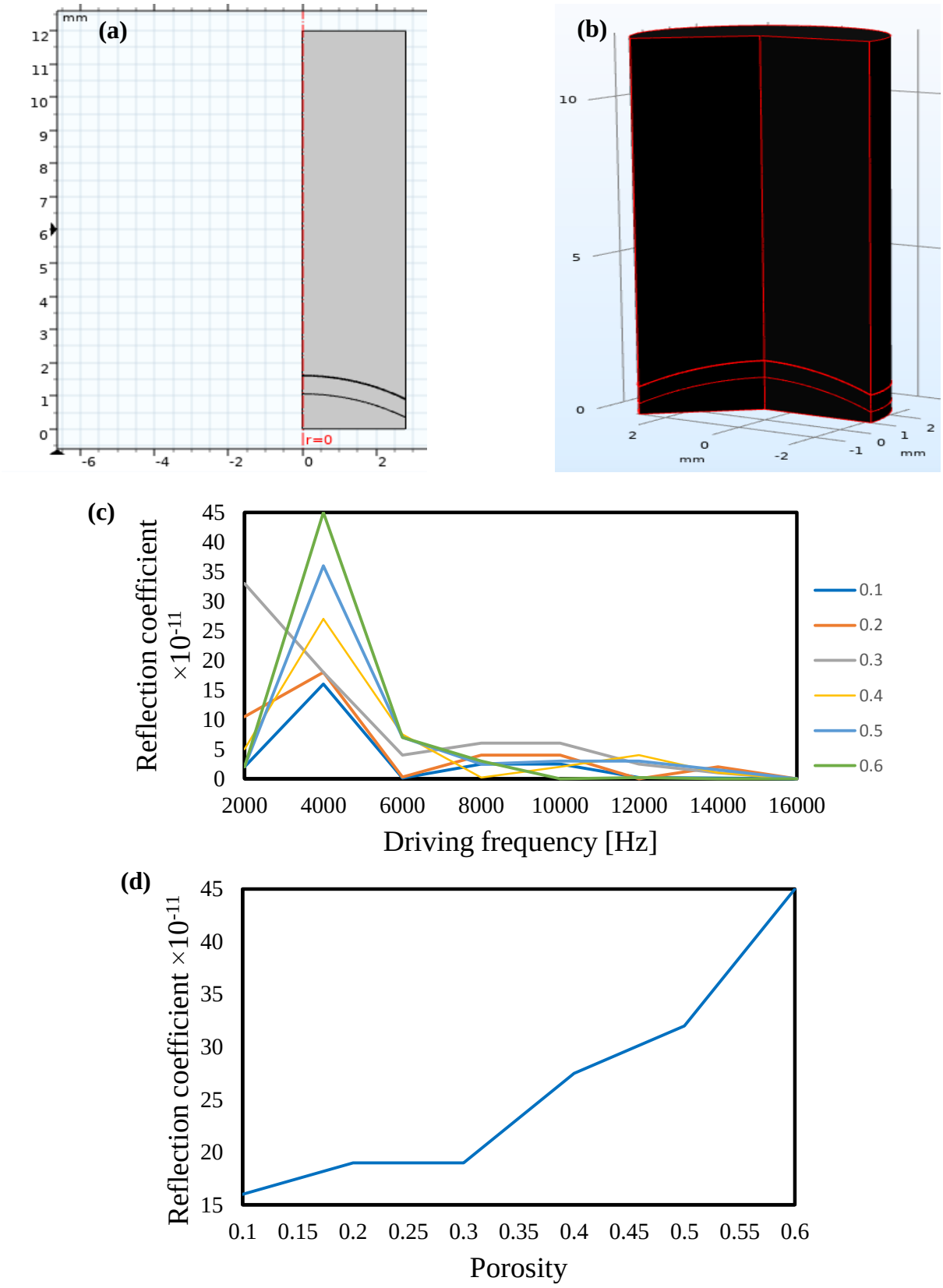

Figure 2. Setup and results for the simulations (a) 2D schematic of simulation model (b) 210° revolution of simulation model (c) graph of reflection coefficient vs driving frequency for porosity 0.1-0.6 (d) graph of reflection coefficient vs porosity at a driving frequency of 4000 Hz

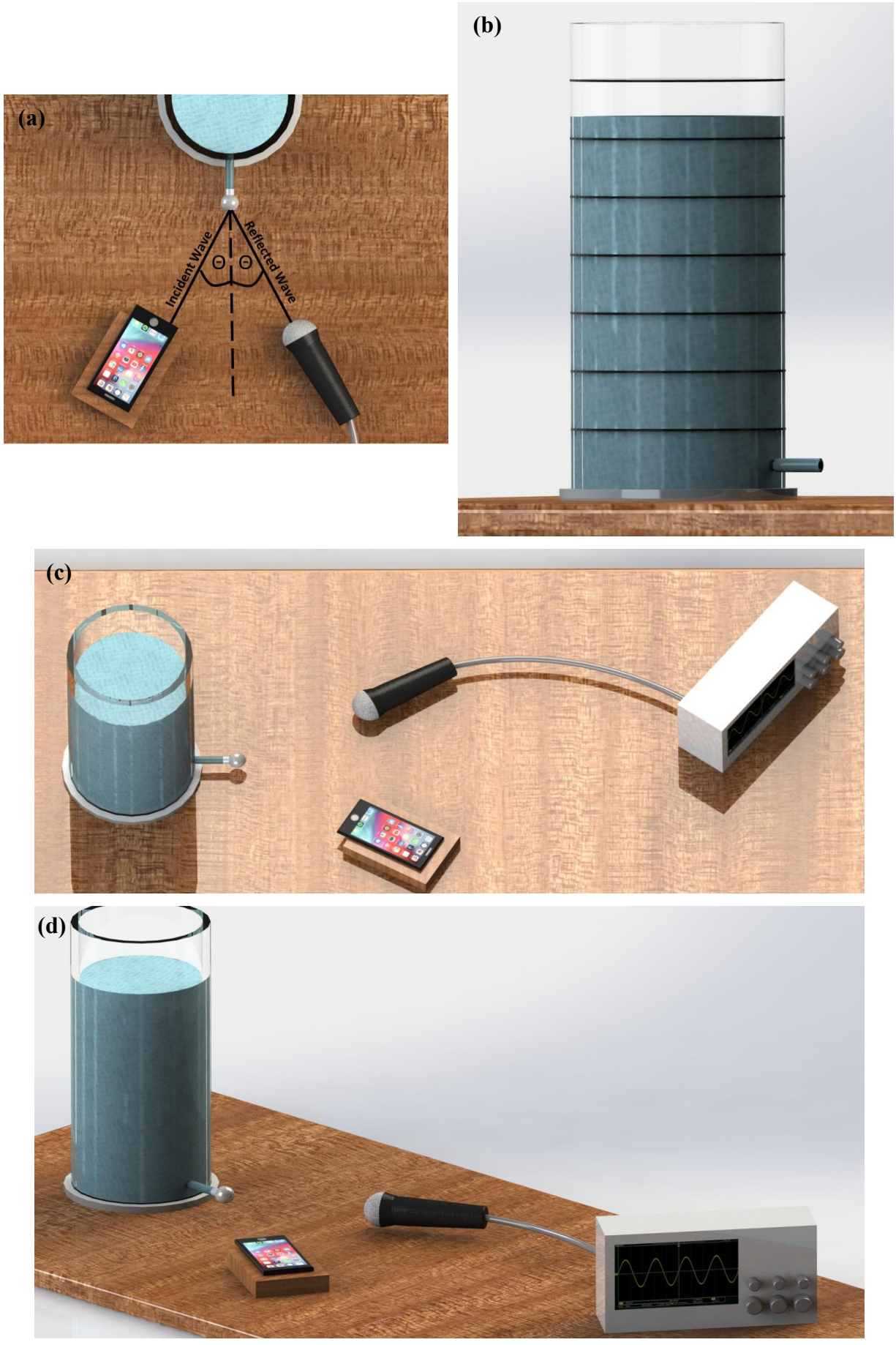

Figure 3. Schematics of the experimental setup produced on SolidWorks (a) Incident vs reflected wave angle (b) Side profile of water tower (c) Diagonal view of the experimental setup (d) Approximate human perspective of experimental setup

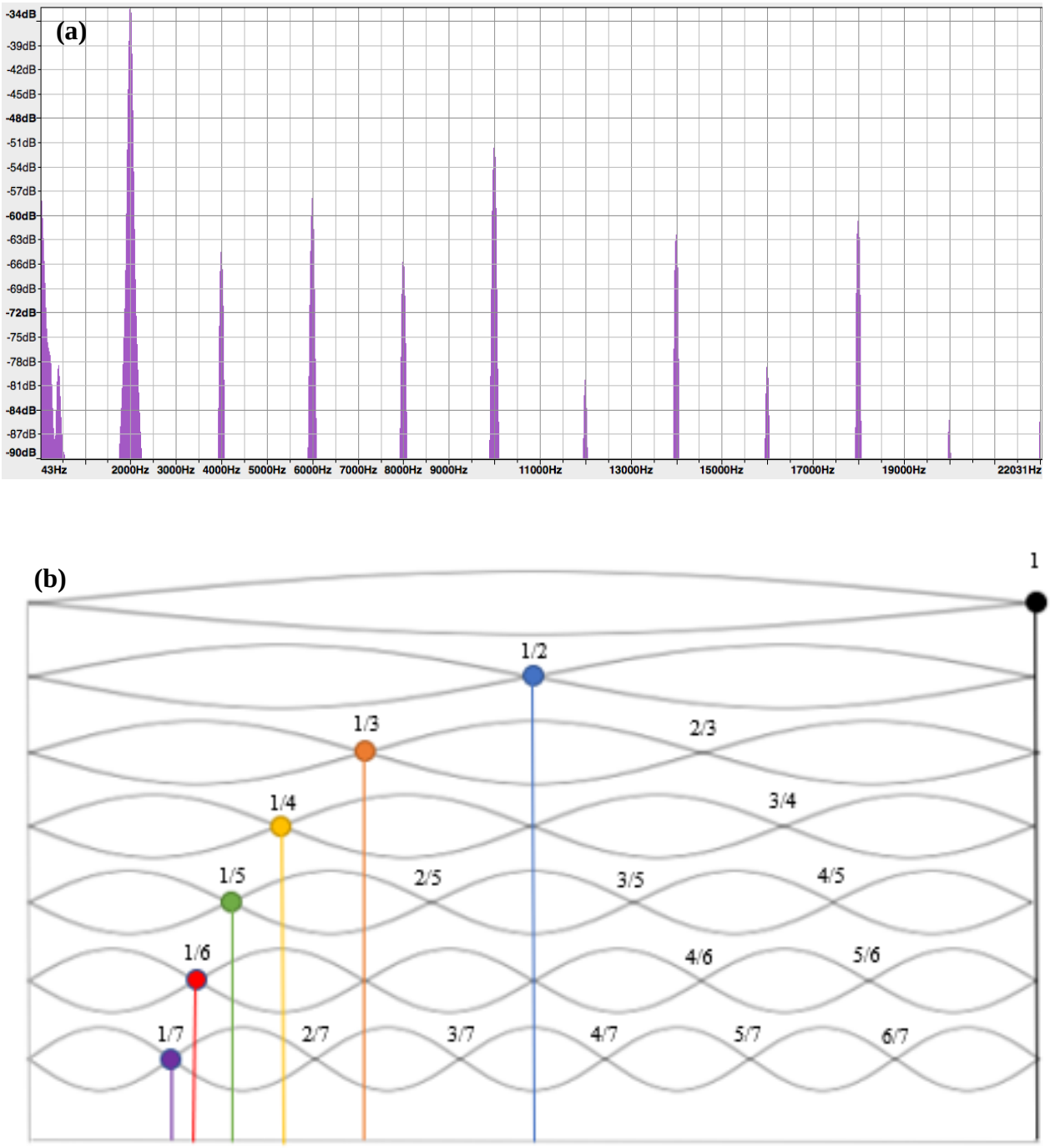

Figure 4. (a) Frequency spectrum for 2000 Hz produced on Audacity (b) Harmonic nodes of sound waves

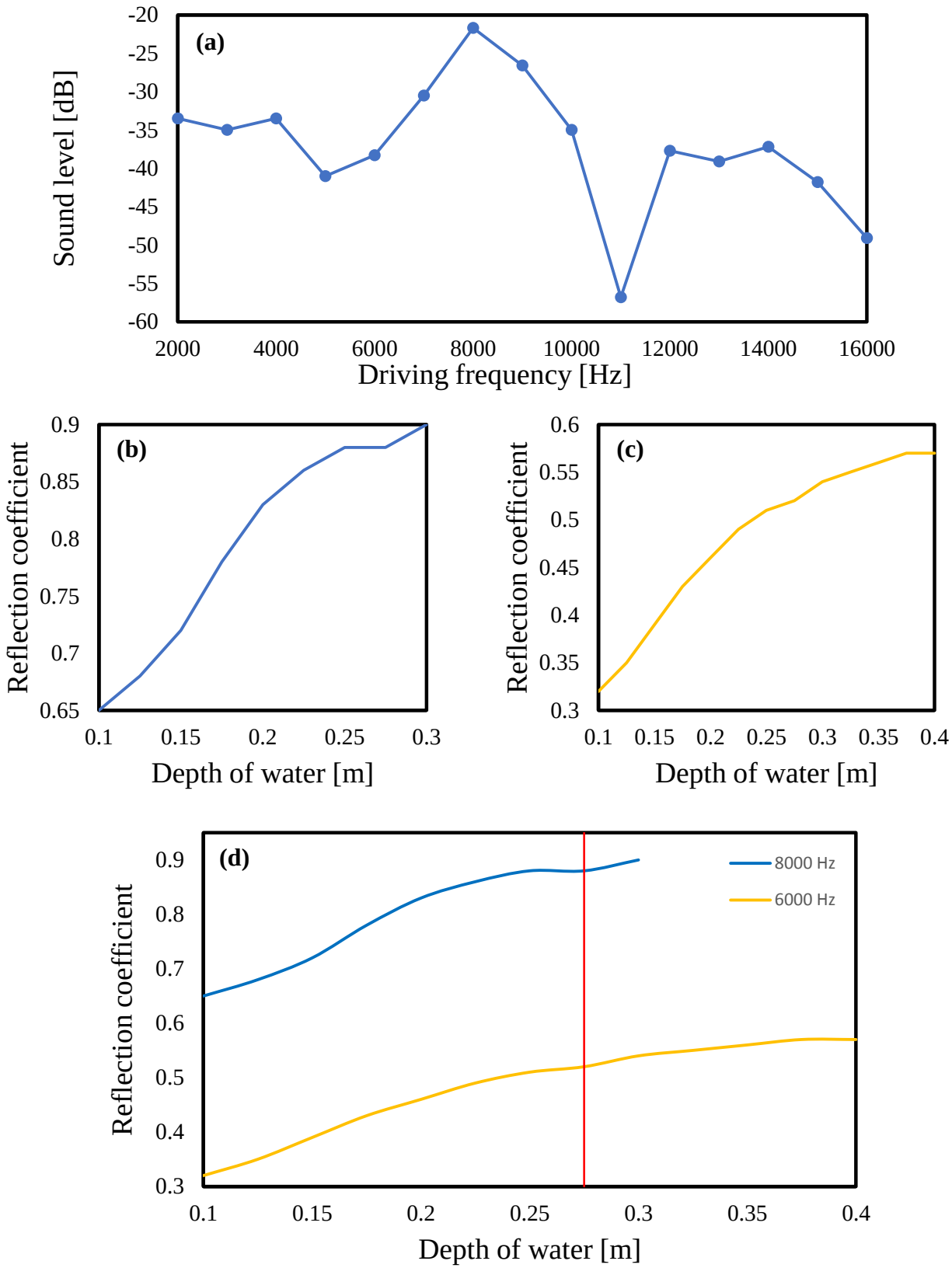

Figure 5. Results of the experiments represented graphically (a) Sound level vs Driving frequency (b) Reflection coefficient vs water depth at 8000 Hz driving frequency (c) Reflection coefficient vs water depth at 6000 Hz driving frequency (d) Reflection coefficient vs water depth comparison between 6000 & 8000 Hz driving frequency

Table 1. Simulation model geometry

Parameter	Value [mm]
Diameter	11.71 [37]
Horizontal corneal curvature	7.87 [38]
Thickness of cornea	0.55 [38]
Thickness of precorneal tear film	0.005

Table 2. Comsol Multiphysics input parameters

Parameter	Value
Driving Frequency sweep	$2000 - 20000\ Hz$ in $1000\ Hz$ increments
Corneal Porosity sweep	$0.1 -\ 0.6$ in 0.1 increments
Density	$1050\ kg.m^{-3}$ [39-40]
Permeability	1.361×10^{-11} [41-42]
Youngs Modulus	$0.208\ MPa$ [43]
Poisson Ratio	0.49 [44]
Bulk Modulus	$3.47 \times\ 10^{6}\ Pa$ [45]
Shear Modulus	$6.98\ \times\ 10^{4}\ Pa$ [45]

Table 3. Driving frequency vs peak sound level

Driving frequency [Hz]	Sound level [dB]
2000	−33.5
3000	−35.0
4000	−33.5
5000	−41.0
6000	−38.3
7000	−30.5
8000	−21.7
9000	−26.6
10000	−35.0
11000	−56.8
12000	−37.7
13000	−39.1
14000	−37.2
15000	−41.8
16000	−49.1

Table 4. Depth of water vs reflection coefficients for a driving frequency of 8000 Hz

Height of water [m]	Sound level 1 [dB]	Sound level 2 [dB]	Sound level 3 [dB]	A_R [dB]
0.100	-27.7	-25.2	-24.5	-25.8 ± 1.7
0.125	-25.6	-23.9	-23.3	-24.3 ± 1.2
0.150	-23.4	-22.6	-23.0	-23.0 ± 0.4
0.175	-21.8	-21.8	-20.6	-21.4 ± 0.7
0.200	-21.4	-19.2	-19.6	-20.1 ± 1.2
0.225	-20.0	-18.7	-19.2	-19.3 ± 0.7
0.250	-19.4	-18.6	-18.7	-18.9 ± 0.4
0.275	-19.1	-18.4	-18.9	-18.8 ± 0.4
0.300	-18.7	-18.4	-18.5	-18.5 ± 0.2

Table 5. Depth of water vs average reflection coefficient for a driving frequency of 8000 Hz

Depth of water [m]	Pressure [Pa]	R_C
0.100	981	0.65
0.125	1226	0.68
0.150	1472	0.72
0.175	1717	0.78
0.200	1962	0.83
0.225	2207	0.86
0.250	2425	0.88
0.275	2698	0.88
0.300	2943	0.90

Table 6. Depth of water vs reflection coefficients for a driving frequency of 6000 Hz

Height of water [m]	Sound level 1 [dB]	Sound level 2 [dB]	Sound level 3 [dB]	A_R [dB]
0.100	-46.4	-52.3	-51.3	-50.0 ± 2.6
0.125	-42.6	-48.0	-46.4	-45.7 ± 2.3
0.150	-39.9	-43.9	-40.6	-41.5 ± 1.7
0.175	-36.0	-39.2	-36.5	-37.2 ± 1.4
0.200	-34.1	-36.5	-33.9	-34.8 ± 1.2
0.225	-32.1	-34.5	-32.0	-32.9 ± 1.2
0.250	-30.5	-32.9	-31.3	-31.6 ± 1.0
0.275	-28.7	-32.8	-30.9	-30.8 ± 1.7
0.300	-28.2	-30.4	-30.0	-29.5 ± 1.0
0.325	-28.8	-29.8	-28.8	-29.1 ± 0.5
0.350	-28.1	-29.0	-28.6	-28.6 ± 0.4
0.375	-27.8	-28.4	-28.2	-28.1 ± 0.2
0.400	-27.8	-28.2	-28.0	-28.0 ± 0.2

Table 7. Depth of water vs average reflection coefficients for a driving frequency of 6000 Hz

Depth of water [m]	Pressure [Pa]	R_C
0.100	981	0.32
0.125	1226	0.35
0.150	1472	0.39
0.175	1717	0.43
0.200	1962	0.46
0.225	2207	0.49
0.250	2425	0.51
0.275	2698	0.52
0.300	2943	0.54
0.325	3188	0.55
0.350	3434	0.56
0.375	3679	0.57
0.400	3924	0.57